Bioorganic & Medicinal Chemistry 17 (2009) 4747–4755

Contents lists available at ScienceDirect

Bioorganic & Medicinal Chemistry

journal homepage: www.elsevier.com/locate/bmc

# Minor structural differences of monomethine cyanine derivatives yield strong variation in their interactions with DNA, RNA as well as on their in vitro antiproliferative activity

Ljubica Glavaš-Obrovac [a,b,*], Ivo Piantanida [c,*], Saška Marczi [b], Lozika Mašić [c], Iliana I. Timcheva [d], Todor G. Deligeorgiev [e]

[a] Department of Medical Chemistry and Biochemistry, School of Medicine, J. J. Strossmayer University of Osijek, 31000 Osijek, Croatia
[b] Department of Nuclear Medicine and Radiation Protection, University Hospital Osijek, 31000 Osijek, Croatia
[c] Division of Organic Chemistry and Biochemistry, Ruđer Bošković Institute, PO Box 180, 10002 Zagreb, Croatia
[d] Institute of Organic Chemistry with Centre of Phytochemistry, Bulgarian Academy of Sciences, 1113 Sofia, Bulgaria
[e] Faculty of Chemistry, University of Sofia, 1, James Bourchier Avenue, 1164 Sofia, Bulgaria

ARTICLE INFO

*Article history:*
Received 17 February 2009
Revised 19 April 2009
Accepted 22 April 2009
Available online 6 May 2009

*Keywords:*
Monomethine cyanines
DNA/RNA binding
Cytotoxicity
Human normal and tumour cells
Cellular uptake

ABSTRACT

Comparison of binding properties of a series of monomethine cyanine derivatives to ds-DNA and ds-RNA revealed significant impact of the properties of substituent attached to the longer axis of aromatic core. Namely, it seems that only compounds **7**, **8** characterised by length of longer axis not exceeding the length of longer axis of basepairs could intercalate into ds-DNA and ds-RNA, while the increased substituent length and additional possibility of hydrogen bonds formation directed binding of **1–6** into ds-DNA minor groove. Consequent ds-RNA over ds-DNA selectivity of **7** and **8** is the most appealing and rather rare property among small molecules. The interactions of **1–8** with ss-RNA were strongly dependent on both, structure of compound and base composition of RNA. The cytotoxicity screening of compounds 1–8 by MTT test revealed considerable antiproliferative activity against solid tumours and especially toward haematological malignancies ($IC_{50}$ = 0.001–6.6 μM), whereby normal human aortic endothelial cells (HAEC) were significantly less affected ($IC_{50}$ = 1–200 μM). The cells of chronic myeloid leukaemia in blast crisis (K562) were especially sensitive to all tested compounds ($IC_{50}$ = 0.001–0.6 μM), while normal lymphocytes were more resistant ($IC_{50}$ = 0.01–1 μM). Results of uptake and intracellular distribution of compounds **1** and **2** in the living cells showed that they do not bind primarily to nuclear DNA but their fluorescence is scattered through the whole cells. A detailed mechanism of antitumor activity of tested molecules remains to be investigated.



## 1. Introduction

Steady state and dynamic fluorescent techniques have been significantly developed during the last two decades and now are in position to represent about 60% of the detection enabling technologies used in molecular biology and medicine.[1] The reason for this hegemony originates from two intrinsic properties of fluorescence: (i) extremely high sensitivity and (ii) high content of the fluorescent signal.

Fluorescence detection is widely used in medical assays and DNA analysis. The intrinsic fluorescence from DNA is very weak and almost all methods for detecting DNA rely on the use of various types of fluorescent probes. The fluorophores interact with DNA covalently and non-covalently to allow polynucleotide detection on gels,[2,3] DNA sequencing,[4–7] fluorescence in situ hybridization[8,9] and for reading of DNA arrays for gene expression.[10,11]

In general, there are three main modes of non-covalent binding of small molecules to DNA/RNA, (i) minor groove binding, (ii) intercalation and (iii) electrostatic interaction of highly positively charged molecules with nucleotide phosphate backbone.[12] Many authors combined more modes of interaction in the same molecule targeting very specific goals. Quite often secondary structure of polynucleotide was applied as recognition modulator, for example structural differences between DNA minor groove (deep, narrow, hydrophobic)[13] and RNA minor groove (broad, shallow)[13] yielded the most extensively studied class of small molecules specifically binding to DNA. Moreover, size of aromatic moiety as well as bulkiness of attached substituents and their ability to also interact non-covalently with polynucleotide could control intercalation ability as well as orientation of intercalated molecule.[14] Several small molecules are known to even switch binding mode from minor

* Corresponding authors. Tel.: +385 1 45 71 210; fax: +385 31 512 227 (L.G.-O.), fax: +385 1 46 80 195 (I.P.).
*E-mail addresses:* glavas-obrovac.ljubica@kbo.hr (L. Glavaš-Obrovac), pianta@irb.hr (I. Piantanida).

0968-0896/$ - see front matter © 2009 Elsevier Ltd. All rights reserved.
doi:10.1016/j.bmc.2009.04.070

groove binding (DNA) to intercalation (RNA).[14] Therefore, fine tuning of structural features of small molecules proved to be powerful tool for control of mode of interaction with DNA/RNA, consequently yielding pronounced impact on the stability and spectroscopic properties of complexes formed.[12]

During the last decade we have investigated novel derivatives of monomethine cyanine dyes and their homodimers based mainly on thiazole orange (TO) and oxazole yellow (YO) chromophores as non-covalently binding nucleic acid fluorogenic probes.[15] The synthesis of here studied monomethine cyanines, which chromophores differ from these of TO and YO, and their fluorescent properties in the presence of double stranded DNA as well have been published recently.[16] Intriguing results, like exceptionally strong fluorescence increase of compounds **1** and **4** (Scheme 1)[16] induced by interaction with DNA prompted us to study in more detail interactions of complete series of compounds with double stranded and single stranded polynucleotides. Moreover, since most of DNA/RNA active species reveal considerable biological activity[17], here we present the in vitro antiproliferative properties of studied compounds on human normal cells and a series of tumour cell lines, whereby the strong fluorescence of some compounds upon binding to target macromolecule was employed to monitor live cell entering rate and intracellular distribution.

## 2. Results and discussion

### 2.1. Physical and chemical properties of aqueous solutions of studied compounds

Compounds **1–8** are moderately soluble in pure water (up to $c = 1 \times 10^{-3}$ mol dm$^{-3}$) and in buffer system used (pH 7, sodium cacodylate/HCl buffer, $I = 0.05$ mol dm$^{-3}$). Aqueous solutions of **1–8** revealed about 5% decrease in the UV/vis spectra when stored in the dark at 8 °C for two weeks. The absorbencies of buffered aqueous solutions of **1–8** are proportional to their concentrations up to $c = 3–4 \times 10^{-5}$ mol dm$^{-3}$, changes of the UV/vis spectra on the temperature increase up to 85 °C were small and reproducibility of UV/vis spectra upon cooling back to 25 °C was within 5% of the spectrum before heating. All mentioned is indicating that **1–8** do not aggregate by intermolecular stacking at experimental conditions used. Aqueous solutions of **1–6**, **8** exhibit weak fluorescence emission at $c = 10^{-6}$ mol dm$^{-3}$ concentrations, while only **7** at these conditions does not emit fluorescence.

### 2.2. Interactions of studied compounds 1–8 with double stranded ds-DNA and ds-RNA in aqueous medium

#### 2.2.1. Fluorimetric titrations

Addition of any double stranded (ds-) polynucleotide resulted in strong increase of fluorescence emission of **1–6**, **8** (example see Figs. 1 and 2). The only exception was **7** exhibiting virtually no fluorescence change upon addition of any ds-DNA or ds-RNA. Processing of the fluorimetric titration data by Scatchard equation[18] gave binding constants (log $K_s$) (Table 1).

Obtained binding constants reveal comparable affinity of **1–6**, **8** toward ct-DNA (Table 1). However, fluorescence of most compounds increased almost linearly with the increase of concentration of poly A–poly U in the biologically relevant range (up to $c = 1 \times 10^{-4}$ mol dm$^{-3}$), pointing toward either low stability of complexes (log $K_s < 4$) or agglomeration of dye molecules along ds-RNA, which is driven by hydrophobic effects. In the latter case dominant interaction of studied compounds would be aromatic stacking interaction between molecules of compound, which would significantly reduce mobility around the methine bridge resulting in fluorescence increase. The only exception was titration of **8** with poly A–poly U (Fig. 2), which yielded log $K_s$ value significantly higher than obtained for any other compound. Moreover, **8** revealed an order of magnitude stronger affinity toward poly A–poly U in comparison with ct-DNA.

#### 2.2.2. Thermal denaturation experiments

Addition of **1–8** induced weak to moderate stabilization of ct-DNA double helix (Table 2), but observed differences in $\Delta T_m$ values could not be correlated to the differences in the structure of compounds. At variance to DNA, most of compounds (**1–6**) did not cause any stabilisation of poly A–poly U. Most intriguingly, compounds **7** and **8** stabilised poly A–poly U exceptionally strong (Table 2). Study of the effect of **8** on the thermal stabilisation of poly A–poly U in more detail revealed strongly nonlinear dependence of $\Delta T_m$ values on the ratio $r$, suggesting saturation of binding sites at $r = 0.1–0.2$ (Fig. 3). Stronger stabilization effect of **8** on poly A–poly U than ct-DNA agrees well with differences in binding constants (Table 1).

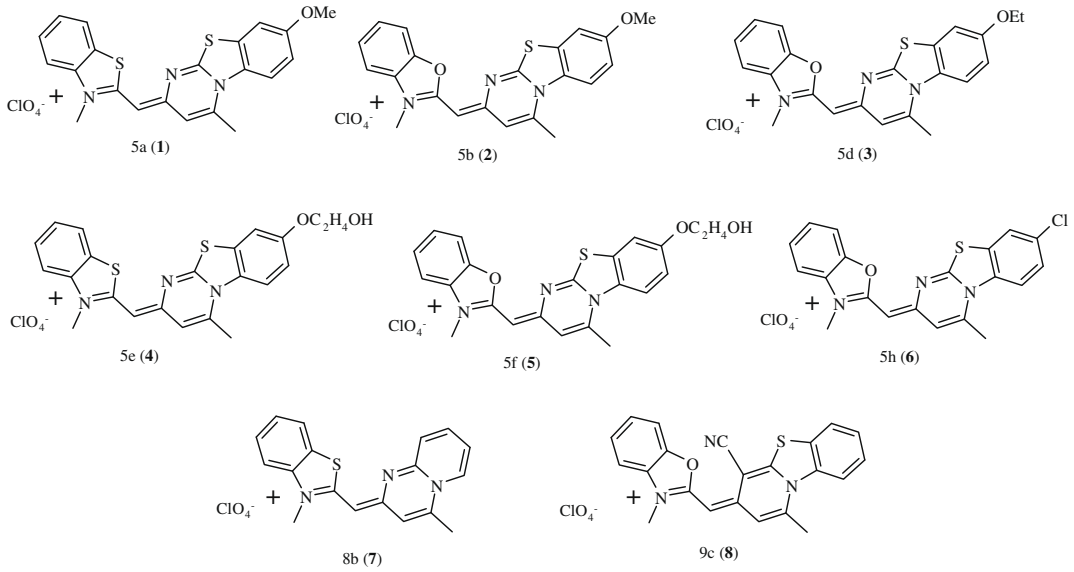


**Scheme 1.** Studied compounds **1–8**.

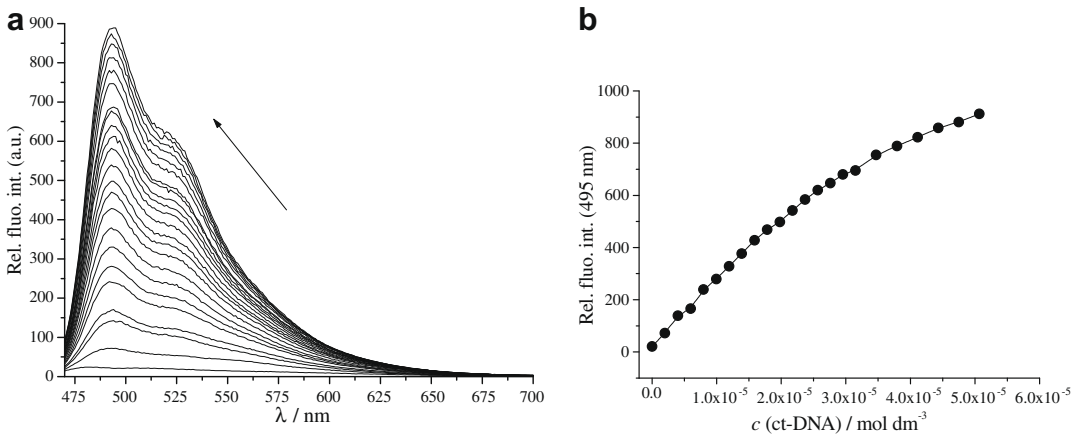


**Figure 1.** (a) Changes in fluorescence spectrum of **8** ($c = 1.67 \times 10^{-6}$ mol dm$^{-3}$, $\lambda_{exc} = 450$ nm) upon titration with ct-DNA; (b) dependence of fluorescence emission at $\lambda_{max} = 495$ nm on $c$(ct-DNA), at pH 7, sodium cacodylate buffer, $I = 0.05$ mol dm$^{-3}$.

### 2.3. Study of interactions of 1–8 with single stranded (ss-) RNA in aqueous medium

Chosen single stranded (ss-) RNA homo-polynucleotides poly A, poly G, poly C, poly U differ significantly not only by nucleobase composition but also by secondary structure. Because of that one could expect that **1–8** would bind by different affinity and binding mode to each of studied homo-polynucleotides, consequently exhibiting strongly dependent fluorescence changes.

The compound **7** exhibited virtually no fluorescence change upon addition of any ss-RNA, therefore it is not discussed in further text. Fluorescence emission of all studied compounds increased almost linearly with the increase of poly C and poly U in concentration up to $1 \times 10^{-4}$ mol dm$^{-3}$, pointing toward either low stability of complexes ($\log K_s << 4$) or agglomeration of dye molecules along ss-RNA driven by hydrophobic effects. Similar changes were observed upon titration of **1–6** with poly A. Actually, only titration of **8** with poly A resulted in strongly non-linear fluorescence changes, which allowed calculation[18] of binding constant ($\log K_s = 6.2$) and Scatchard ratio $r_{[\text{bound } \mathbf{8}]/[\text{polynucleotide}]} = 0.18$ (Fig. 4).

At variance to other ss-RNAs', titrations with poly G yielded strongly non-linear fluorescence change of all studied compounds (Fig. 5, Supplementary data). However, titration curves were mostly of sigmoidal shape, pointing toward either: (a) co-existence of several different binding modes; or (b) cooperative binding of compounds to poly G. Consequently, it was not possible to fit titration data to non-cooperative Scatchard equation.[18] Whatever the reason might be, all titrations were completed at about $r_{[\text{compound}]/[\text{poly G}]} = 0.1$ and $c(\text{poly G}) = 1.5 \times 10^{-5}$ mol dm$^{-3}$, pointing toward very high cumulative affinity ($\log K_s > 6$) of studied compounds toward poly G.

**Table 1**
Binding constants ($\log K_s$)[a] of **1–6**, **8** calculated from the fluorimetric titrations with polynucleotides at pH 7.0 (buffer Na cacodylateag, $I = 0.05$ mol dm$^{-3}$)

| | ct-DNA | | poly A–poly U | |
|---|---|---|---|---|
| | Log $K_s$ | [b]Int/Int$_0$ ($\lambda$/nm) | Log $K_s$ | [b]Int/Int$_0$ ($\lambda$/nm) |
| **1** | 4.5 | 56 (495 nm) | 4.2 | 900 (531 nm) |
| **2** | 5.0 | 16.7 (530 nm) | [d] | [d] |
| **3** | 4.7[c] | 63 (512 nm)[c] | 4.5[d] | 50(510 nm) |
| **4** | 4.8[c] | 38 (530 nm)[c] | 4.5[d] | 1000 (530 nm) |
| **5** | 4.6 | 42 (533 nm) | 4.3 | 93 (510 nm) |
| **6** | 4.6 | 60 (514 nm) | 4.5 | 310 (511 nm) |
| **8** | 5.1 | 977 (496 nm) | 6.8 | 460 (495 nm) |
| | | | | 270 (521 nm) |

[a] Processing of titration data by means of Scatchard equation[18] gave values of ratio $n_{[\text{bound compound}]/[\text{polynucleotide}]} = 0.3–0.1$, for easier comparison all $\log K_s$ values were re-calculated for fixed $n = 0.2$.
[b] Int$_0$—starting fluorescence intensity of compound; Int—fluorescence intensity of compound/polynucleotide complex calculated by Scatchard equation.[18]
[c] Only estimated due to the mixed binding modes.
[d] Only estimated due to the increase of fluorescence proportional to $c$(compound) due to low affinity toward polynucleotide or other effects.

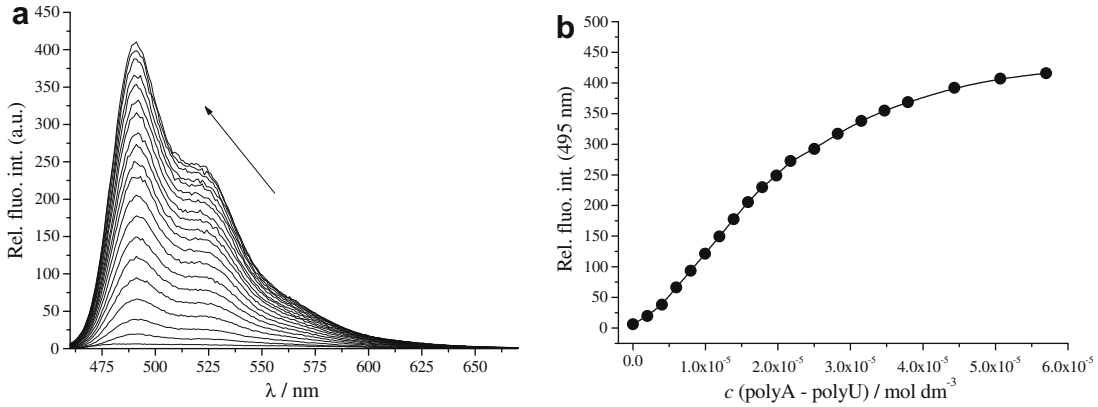


**Figure 2.** (a) Changes in fluorescence spectrum of **8** ($c = 1.67 \times 10^{-6}$ mol dm$^{-3}$, $\lambda_{exc} = 450$ nm) upon titration with poly A–poly U; (b) dependence of fluorescence emission at $\lambda_{max} = 495$ nm on $c$(poly A–poly U), at pH 7, sodium cacodylate buffer, $I = 0.05$ mol dm$^{-3}$.

**Table 2**
The [a,b]$\Delta T_m$ values (°C) of studied ds-polynucleotides upon addition of studied compounds at pH 7 (buffer sodium cacodylate, $I$ = 0.05 mol dm$^{-3}$)

| | 1 | 2 | 3 | 4 | 5 | 6 | 7 | 8 |
|---|---|---|---|---|---|---|---|---|
| ct-DNA | 3.0 | 2.7 | 4.0 | 1.3 | 0.8 | 1.0 | 1.9 | 4.1 |
| polyA–polyU | 0 | 0 | 0 | 0 | 0 | 0 | 10.4 | 19.5<br>15.3 ([b]$r$ = 0.1);<br>18.4 ([b]$r$ = 0.2) |

[a] Error in $\Delta Tm$: ± 0.5 °C.
[b] $r_{[compound]/[polynucleotide]}$ = 0.3.

## 2.4. Discussion of DNA/RNA binding results

Fluorimetric titrations and thermal denaturation experiments point out that **1–8** significantly interact with calf thymus ds-DNA. On the other hand, thermal denaturation experiments of poly A–poly U revealed that compounds **1–6** do not thermally stabilize ds-RNA at biologically relevant conditions, whereby the strong fluorescence increase of **1–6** in titration experiments was most likely caused by interactions between molecules of **1–6** inside one of hydrophobic ds-RNA grooves. However, in contrast to **1 – 6** and the most appealing was extraordinary strong thermal stabilisation of poly A–poly U by **7** and **8**, pointing toward strong binding affinity of only these two compounds with ds-RNA. Moreover, $\Delta T_m$ values of poly A–poly U induced by addition of **7** and **8** were about five times higher than those measured for ct-DNA, which corresponds nicely to an order of magnitude higher log $K_s$ value calculated for **8**/ poly A–poly U complex in respect to **8**/ct-DNA complex. Such ds-RNA over ds-DNA preference is very rare among low molecular weight molecules.[12,14]

Comparison of structures of **1–8** and their interactions with ds-DNA and ds-RNA pointed toward several interesting features. Model in the Figure 6 (right side) was prepared by retrieving the crystal structure of ethidium bromide (EB)–cytidylyl(3′-5′) guanosine dinucleoside[19] and replacing the intercalated EB with aromatic core of **1–8**—two condensed aromatic units connected by methine bridge—which are characterised by the length over longer axis of about 11.3 Å (compound **7**) or 12.5 Å (compounds **1–6**, **8**). However, various substituents R (Fig. 6, right) elongate some molecules by approximately 3 Å (–O–$CH_3$); 4 Å (–O–$CH_2$–$CH_3$) or 5.3 Å (–O–$CH_2$–$CH_2$–OH). The longer axes of common DNA/RNA intercalators are significantly shorter, e.g. ethidium bromide overall length is 10.6 Å (Fig. 6). The larger molecules like porphyrin (e.g., $TMPyP^{4+}$, approx. 16 Å/9 Å, Fig. 6) are often border cases, which intercalate into DNA/RNA only at specific conditions.[14,20] Since the length of a DNA/RNA basepair longer axis is about 11–12 Å (Fig. 6), only compounds **7** and **8** with no substituent R are able to fit into the polynucleotide double strand with longer axis coplanar to longer axes of basepairs, which again is essential for efficient aromatic stacking interactions. Other studied compounds (**1–6**) can either: (a) intercalate tilted at some angle in respect to the longer axes of basepairs, which would diminish aromatic stacking interactions; or (b) bind into one of the grooves of ds-DNA/RNA, whereby aromatic moieties of **1–8** can form several hydrogen bonds within the DNA minor groove and even more, some of substituents (e.g., R = (–O–$CH_2$–$CH_2$–OH)) are able to form additional binding inter-

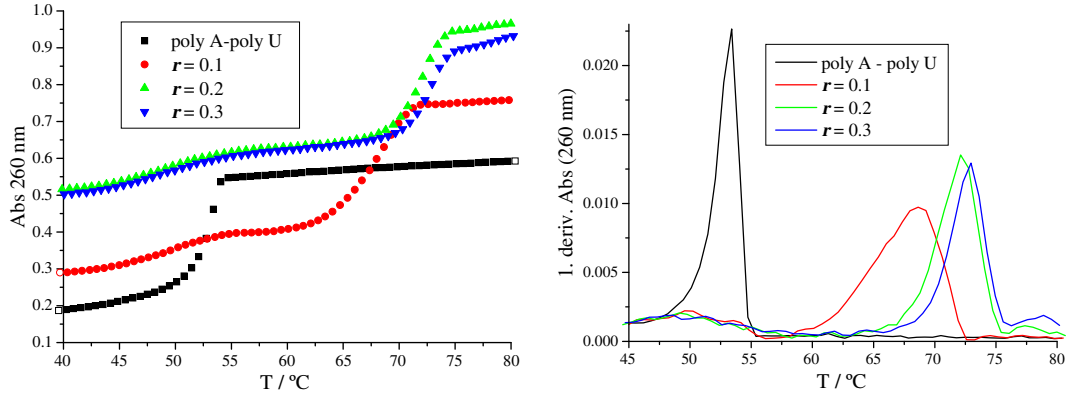


**Figure 3.** Thermal denaturation curves of poly A–poly U upon addition of different ratios of **8** at pH 7 (sodium cacodylate buffer, $I$ = 0.05 mol dm$^{-3}$).

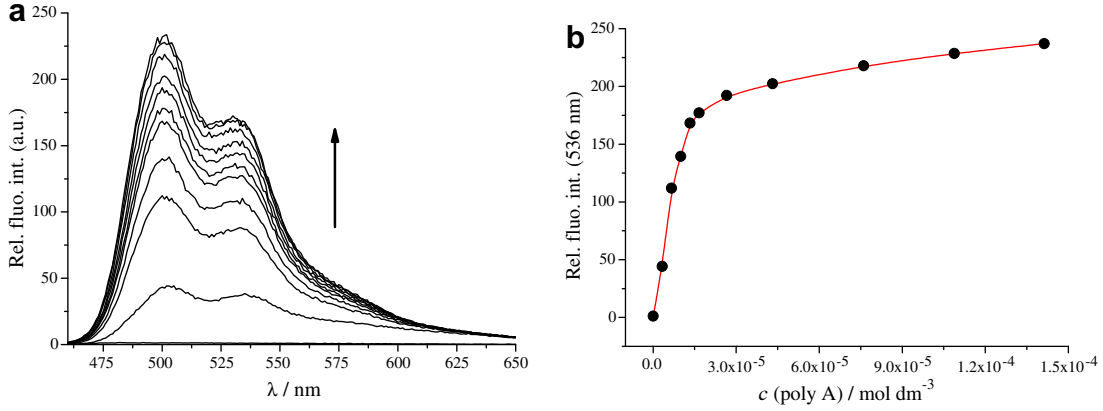


**Figure 4.** (a) Changes in fluorescence spectrum of **8** ($c$ = 1.67 × 10$^{-6}$ mol dm$^{-3}$, $\lambda_{exc}$ = 450 nm) upon titration with poly A; b) Dependence of fluorescence emission at $\lambda_{max}$ = 536 nm on $c$(poly A), at pH 7, sodium cacodylate buffer, $I$ = 0.05 mol dm$^{-3}$.

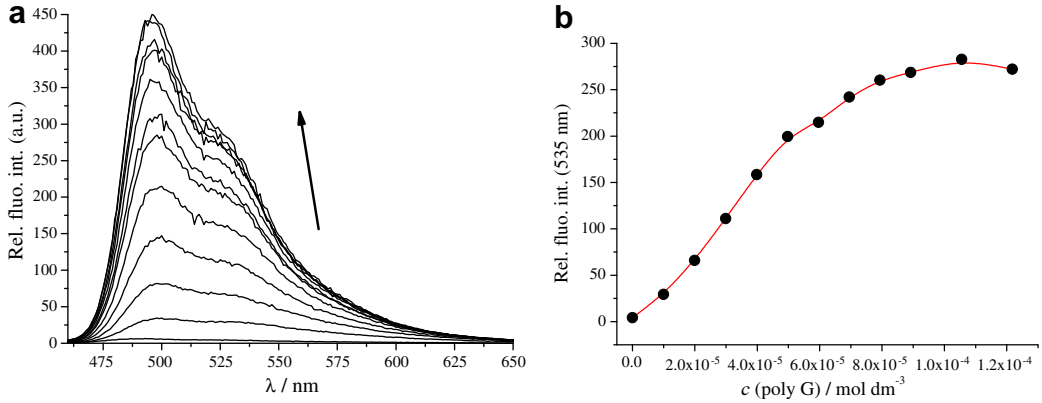


**Figure 5.** (a) Changes in fluorescence spectrum of **8** ($c = 1.67 \times 10^{-6}$ mol dm$^{-3}$, $\lambda_{exc} = 450$ nm) upon titration with poly G; (b) dependence of fluorescence emission at $\lambda_{max} = 536$ nm on $c$(poly G), at pH 7, sodium cacodylate buffer, $I = 0.05$ mol dm$^{-3}$.

actions. The latter binding mode is strongly supported for compounds **1–6** by their exclusive thermal stabilisation of ds-DNA but not ds-RNA, which is characteristic for minor groove binding.[14] At variance to compounds **1–6**, 'shorter' compounds **7** and **8** most likely intercalate into both, ds-DNA and ds-RNA. The stronger thermal stabilisation ds-RNA than ds-DNA by **7** and **8** agrees well with the selectivity of ethidium bromide.[14]

Further on, fluorimetric titrations suggest that **1–8** do not form strong complexes with pyrimidine (U and C) ss-RNA under biologically relevant conditions. The same conclusion is valid for **1–7** and poly A with the exception of **8**, which forms extraordinary stable complex. Most intriguingly, all studied compounds strongly interact with poly G, yielding sigmoidal fluorimetric titration curves. Although the binding mode(s) is/are not clear yet, such specificity of studied compounds toward poly G in respect to other ss-RNA could be attributed to peculiar secondary structures poly G could form.[13]

## 2.5. In vitro activity of studied compounds on human normal and tumour cells

Most of small molecules which interact strongly with isolated double stranded (ds-) DNA, show pronounced biological activity, often based on binding to cellular DNA.[21] Therefore it was of high interest to determine the *in vitro* antiproliferative potential of here presented compounds **1–8**.

### 2.5.1. Cytotoxic effect of compounds 1–8

Studied monomethine cyanine derivatives **1–8** reveal large variation in cytotoxic effects against normal cells and tumour cell lines, depending not only on the type of the cells and dose of the tested compound, but also on the compound structure. In addition, morphological changes in treated cells were also observed, whereby cells became smaller, round and absolute number of the cells is lower in comparison with non-treated cells.

According to the results of antiproliferative screening tests summarised in Table 3, compounds **1–8** demonstrated very good inhibitory activity with $IC_{50}$ ranging from 0.1 to 100 μM on human solid tumour cells. In the same experimental settings normal human aortic endothelial cells (HAEC) were more resistant ($IC_{50}$ range achieved on HAEC cells was between 1–200 μM). Compounds **1**, **2**, and **3**, have stronger inhibitory potency on the solid tumour cells growth when compared to other compounds tested, whereby their profile of growth inhibitory activity is very similar.

The chronic myeloid leukaemia in blast crisis (K562) cells was especially sensitive to the **1–8** ($IC_{50}$ range was between 0.001

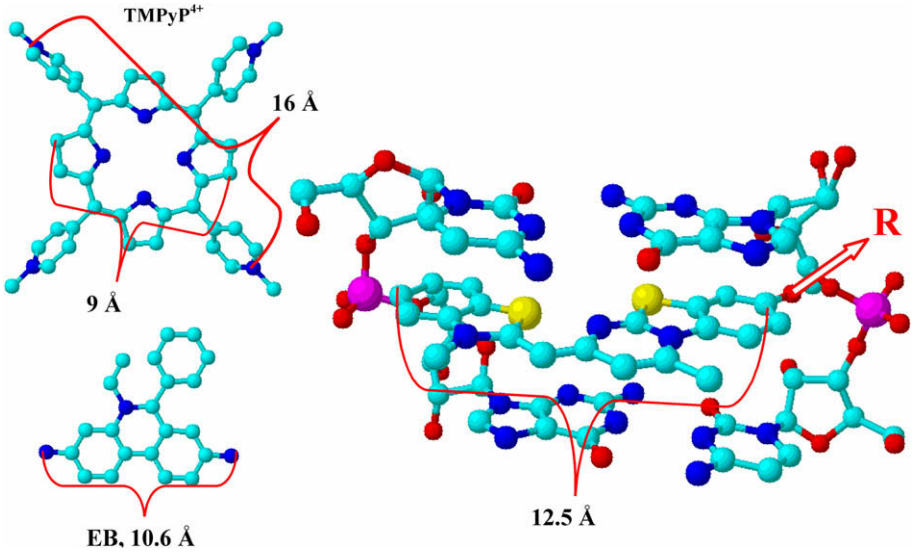


**Figure 6.** A drawing representing: left: structures of $TMPyP^{4+}$ and ethidium bromide (EB). Right: a model of aromatic core of **1–6**, **8** (two condensed aromatic units connected by methine bridge) inserted between basepairs of modified crystal structure[19] instead of ethidium bromide, whereby the R denotes various substituents—here presented intercalator orientation is only the most probable possibility that would explain the influence of **R** on a switch of binding mode.

**Table 3**
Sensitivity of human tumour and normal cells to compounds **1–8**

| Cells | IC50 (μM) | | | | | | | |
|---|---|---|---|---|---|---|---|---|
| | **1** | **2** | **3** | **4** | **5** | **6** | **7** | **8** |
| *Solid tumour* | | | | | | | | |
| SW-620 | 0.2 ± 0.07 | 0.6 ± 0.09 | 0.1 ± 0.07 | 0.55 ± 0.24 | 5.2 ± 1.29 | 5.8 ± 0.35 | 7.0 ± 1.07 | 6.8 ± 0.84 |
| HT-29 | 0.5 ± 0.12 | 0.5 ± 0.07 | 0.6 ± 0.10 | 1.1 ± 0.14 | 7.2 ± 2.5 | 5.1 ± 0.49 | 5.2 ± 0.90 | 5.9 ± 0.05 |
| CaCo2 | 0.8 ± 0.01 | 1.0 ± 0.01 | 0.8 ± 0.22 | >100 | 40 ± 11.3 | 8.2 ± 0.02 | 10.1 ± 1.1 | 9.6 ± 1.07 |
| HeLa | 0.5 ± 0.04 | 2.1 ± 0.20 | 2.0 ± 0.71 | 80 ± 14.30 | 80 ± 14.7 | 3.9 ± 0.91 | 9.9 ± 0.50 | 8.2 ± 0.65 |
| MIAPaCa2 | 0.06 ± 0.01 | 0.5 ± 0.41 | 0.1 ± 0.04 | 0.51 ± 0.05 | 8.5 ± 0.09 | 2.1 ± 0.06 | 1.8 ± 0.28 | 2.2 ± 0.13 |
| HEp-2 | 0.5 ± 0.03 | 0.7 ± 0.21 | 0.5 ± 0.02 | 0.93 ± 0.04 | 6.8 ± 0.05 | 7.0 ± 1.03 | 3.6 ± 0.89 | 5.5 ± 1.00 |
| NCI-H358 | 0.6 ± 0.05 | 0.8 ± 0.18 | 0.1 ± 0.01 | 2.1 ± 0.31 | 9.0 ± 2.12 | 1.1 ± 0.17 | 2.0 ± 0.22 | 2.4 ± 0.05 |
| *Leukemia and lymphoma* | | | | | | | | |
| K562 | 0.001 ± 0.0001 | 0.001 ± 0.00 | 0.001 ± 0.0007 | 0.06 ± 0.003 | 0.07 ± 0.01 | 0.06 ± 0.01 | 0.09 ± 0.02 | 0.05 ± 0.01 |
| Jurkat | 0.1 ± 0.04 | 0.5 ± 0.25 | 0.09 ± 0.01 | 0.9 ± 0.06 | 6.6 ± 1.40 | 0.52 ± 0.16 | 1.3 ± 0.04 | 3.9 ± 0.07 |
| HuT78 | 0.01 ± 0.006 | 0.1 ± 0.03 | 0.05 ± 0.003 | 0.5 ± 0.04 | 0.7 ± 0.12 | 0.06 ± 0.01 | 0.2 ± 0.02 | 0.5 ± 0.23 |
| *Normal* | | | | | | | | |
| HAEC | 3.3 ± 0.9 | 1.1 ± 0.25 | 1.0 ± 0.54 | >200 | 70 ± 9.35 | 50.3 ± 3.4 | 9.6 ± 0.44 | 50.1 ± 6.1 |
| Lymphocytes | 0.1 ± 0.02 | 0.04 ± 0.32 | 0.01 ± 0.006 | 1.2 ± 0.07 | 0.59 ± 0.07 | 0.09 ± 0.02 | 0.6 ± 0.02 | 0.1 ± 0.26 |

$IC_{50}$—Drug concentration that inhibited cell growth by 50%. Data represent mean $IC_{50}$ (μM) values ± standard deviation (SD) of three independent experiments. Exponentially growing cells were treated with substances during 72-h period. Cytotoxicity was analysed using MTT survival assay.

and 0.6 μM). Obtained result is very significant considering the fact that leukaemia and lymphomas are serious malignancies,[22] and K562 cell line, derived from a chronic myeloid leukaemia (CML) patient and expressing antiapoptotic B3A2 bcr-abl hybrid gene, is known to be particularly resistant to most of currently used therapeutics.[23] On the other hand, the $IC_{50}$ range obtained on normal lymphocytes was between 0.01 and 1 μM.

The antiproliferative effect of **4** strongly depended on a type of cells treated, and for solid tumour cell lines varying almost two orders of magnitude. Furthermore, compound **4** has shown the highest selectivity toward some tumour cell lines (SW-620, MIAPaCa2, and HEp-2) compared to normal cells (Table 3), although the origin of such strong selectivity is not clear. Compounds **1** and **4** are also promising candidates showing interesting differential activity toward leukaemia and lymphoma cells in comparison with normal human lymphocytes.

Taking in account structure of **1–4** and their binding potential to DNA and RNA, observed stronger inhibitory effect on the growth of tumour cells in comparison to normal cells could be attributed to the fact that transformed cells have higher proliferative capacity and are more sensitive to malfunction in synthesis of cell's macromolecules.[24] On the other hand, low cytotoxicity of compounds **5–8** could be their advantage in applications like cellular fluorescent probes.

### 2.5.2. Uptake and intracellular distribution of 1 and 2 in the living cells studied by fluorescence microscopy

Intense fluorescence of **1–6**, **8** when bound to DNA/RNA (as well as to any other target which will result in loss of mobility around the methine bridge), allowed efficient monitoring of their uptake and distribution in living cells by fluorescence microscopy. Compounds **1** and **2** were chosen for staining experiments as representatives of more biologically active group of studied compounds. Concentrations of **1** and **2** (1.0, 0.1 and 0.01 μM) were chosen according to their cytotoxic effects on treated tumour cell lines (Table 3). In a parallel experiment cells were treated with propidium iodide (PI) but red fluorescence of PI was not observed in any of studied cell lines and under visible light cells didn't show changed morphology. These results strongly support viability of studied cells.

At $c$(**1**, **2**) = 0.01 μM incubation of 120 min was necessary for efficient staining of the living cells (Figs. 7 and 8), and at $c$(**1**, **2**) = 0.1–1 μM cells were nicely stained already within 30–60 min (Fig. 9). The mechanism by which **1** and **2** enter the living cells is unknown at present but due to their low molecular weight and hydrophobic properties well balanced with positive charge, diffusion through cell membrane could be proposed.

Furthermore, contrast staining by DAPI (which selectively accumulates in the cell nucleus) of the cells previously exposed to **1** and **2**, respectively, (Fig. 10) pointed that **1** and **2** do not bind primarily

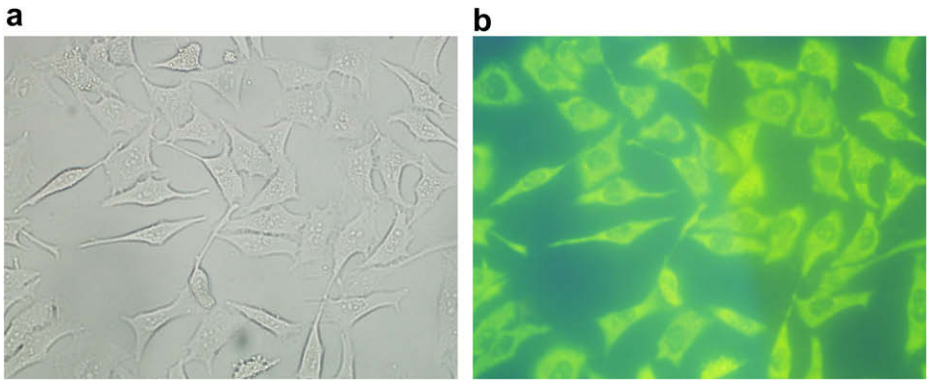


**Figure 7.** HeLa cells stained with 0.01 μM **1** for 120 min and analysed under (a) visible light microscopy; (b) $\lambda_{exc}$ = 450–490 nm, $\lambda_{em}$ = 520 nm, green fluorescence of **1**. Magnification 400×.

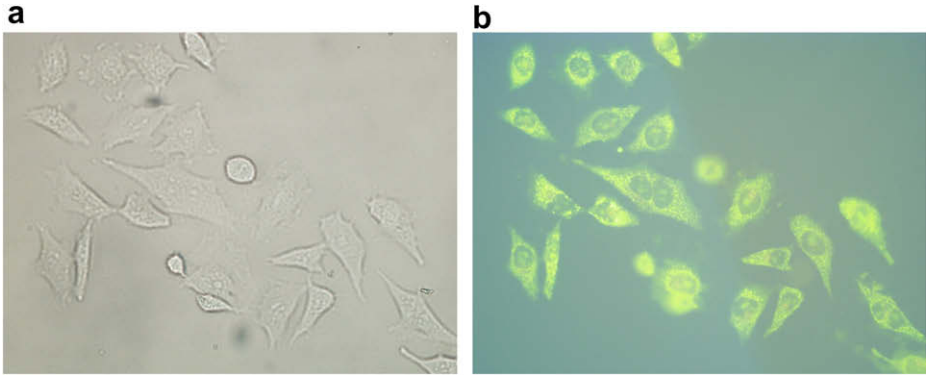


**Figure 8.** HeLa cells stained with 0.01 μM **2** for 120 min and analysed under (a) visible light microscopy; (b) $\lambda_{exc}$ = 450–490 nm, $\lambda_{em}$ = 520 nm, green fluorescence of **2**. Magnification 400×.

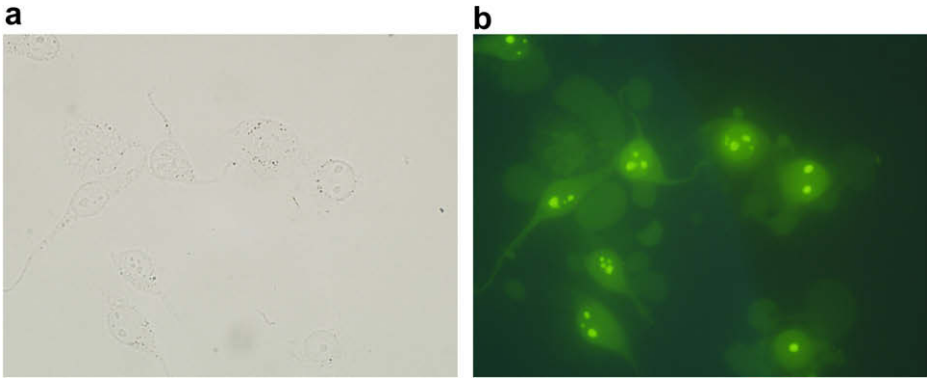


**Figure 9.** HeLa cells stained with 1 μM **2** for 60 min and analysed under (a) visible light microscopy; (b) $\lambda_{exc}$ = 450–490 nm, $\lambda_{em}$ = 520 nm, green fluorescence of **2**. Magnification 630×.

to nuclear DNA but their fluorescence are scattered through the whole cells (Figs. 7–9). Is retaining of investigated compounds in the cytoplasm result of their interaction with mitochondrial DNA, with RNAs, or with other cellular macromolecules should be elucidated.

## 3. Conclusions

Comparison of binding properties of **1–8** to ds-DNA and ds-RNA with compound structures revealed significant impact of the properties of substituent **R** attached to the longer axis of aromatic core (Fig. 6), whereby it seems that the increased length and possibility of multiple hydrogen bond formations lead to exclusive binding of **1–6** into ds-DNA minor groove, while only **7**, **8** (characterised by length of longer axis not exceeding the length of basepair longer axis) could intercalate into both, ds-DNA and ds-RNA. The observed ds-RNA over ds-DNA selectivity of **7** and **8** is the most appealing and rather rare property among small molecules which would be interesting to study in more detail. Furthermore, ds-RNA induced stronger fluorescence increase of the most of studied compounds in comparison with ds-DNA titrations, whereby the fluorescence increase of **1** and **4** upon ds-RNA addition was exceptionally strong. Since **1–6** actually do not thermally stabilize ds-RNA, such a strong fluorescence increase is most likely result of compounds agglomeration and self-stacking within the hydrophobic conditions of ds-RNA grooves.

The interactions of **1–8** with ss-RNA were strongly dependent on both, structure of compound and base composition of RNA.

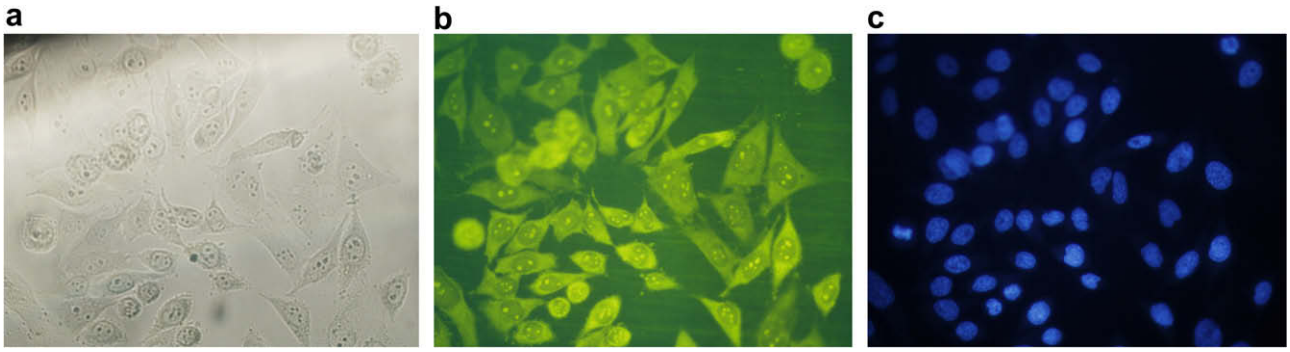


**Figure 10.** HeLa cells were stained with 0.1 μM **1** for 60 min, then washed with PBS and stained with 1 nM DAPI for 3 min: (a) visible light microscopy; (b) $\lambda_{exc}$ = 450–490 nm, $\lambda_{em}$ = 520 nm, green fluorescence of **1**; (c) $\lambda_{exc}$ = 340 nm, $\lambda_{em}$ = 397 nm, DAPI binds selectively to DNA yielding blue fluorescent nuclei. Magnification 400×.

The most intriguing observation was that among studied compounds exclusively **8** formed stable complex with poly A under biologically relevant conditions, whereby the calculated binding constant was surprisingly high. Moreover, **1–6, 8** revealed pronounced interactions with poly G even at μM concentrations, accompanied by exceptionally strong fluorescence increase. Therefore, compounds **1–6, 8** could be considered as highly promising lead compounds toward specific fluorimetric probes for consecutive G-rich single stranded sequences, which could justify further detailed research.

Compounds **1**–**3** are very potent and **4**–**6** rather good inhibitors of the growth of leukaemia and lymphoma cells as well as tumour cells derived from solid tumours. Unlike the response of tumour cells to tested compounds, normal endothelial cells were significantly resistant. The K562 cells derived from serious haematological malignancy, chronic myeloid leukaemia in blast crisis, were especially sensitive to the all tested monomethine cyanine derivatives, which strongly supports additional studies of their mechanism of action on leukaemia and lymphoma cells of different lineages. Furthermore, study of the uptake and intracellular distribution of **1** and **2** in the living cells demonstrated efficient entering of compounds into the cells and binding to the cell's cytoplasm macromolecules. Do studied compounds interact with mitochondrial DNA, with RNAs, or with other cellular macromolecules remain to be investigated.

## 4. Experimental

### 4.1. Spectroscopy and DNA/RNA

The UV/vis spectra were recorded on a Varian Cary 100 Bio spectrophotometer, and fluorescence spectra on a Varian Cary Eclipse spectrophotometer at 25 °C using appropriate 1 cm path quartz cuvettes. For study of interactions with DNA and RNA, aqueous solutions of compounds buffered to pH 7 (sodium cacodylate buffer, $I = 0.05$ mol dm$^{-3}$).

Polynucleotides were purchased as noted: poly A–poly U, poly A, poly G, poly C, poly U (Sigma), *calf thymus* (*ct*)-DNA (Aldrich). Polynucleotides were dissolved sodium cacodylate buffer, $I = 0.05$ mol dm$^{-3}$, pH 7. The calf thymus (*ct*-) DNA was additionally sonicated and filtered through a 0.45 μm filter.[25] Polynucleotide concentration was determined spectroscopically[26] as the concentration of phosphates.

Spectrophotometric titrations were performed at pH 7 (sodium cacodylate buffer, $I = 0.05$ mol dm$^{-3}$) by adding portions of polynucleotide solution into the solution of the studied compound. In fluorimetric experiments excitation wavelength of $\lambda_{exc} > 300$ nm was used to avoid the inner filter effect caused increasing absorbance of the polynucleotide. Emission was collected in the range $\lambda_{em} = 460–700$ nm. Processing of titration data obtained for ds-DNA and ds-RNA by means of Scatchard equation[18] gave values of ratio $n = 0.3–0.1$, but for easier comparison all $K_s$ values were re-calculated for fixed $n = 0.2$. Values for $K_s$ given in Table 1 all have satisfactory correlation coefficients (>0.99). Thermal melting curves for ds-DNA, ds-RNA and their complexes with studied compounds were determined as previously described[26] by following the absorption change at 260 nm as a function of temperature. Absorbance of the ligands was subtracted from every curve and the absorbance scale was normalised. $T_m$ values are the midpoints of the transition curves determined from the maximum of the first derivative and checked graphically by the tangent method.[26] The $\Delta T_m$ values were calculated subtracting $T_m$ of the free nucleic acid from *T*m of the complex. Every $\Delta T_m$ value here reported was the average of at least two measurements. The error in $\Delta T_m$ is ±0.5 °C.

### 4.2. Antiproliferative activity

#### 4.2.1. Cells

The experiments were carried out on 11 human cell lines and 1 primary cell line. The following human cell lines were used: bronchoalveolar carcinoma (NCI-H358), cervical adenocarcinoma (HeLa), laryngeal carcinoma cells (Hep-2), pancreatic carcinoma cells (MIAPaCa2), colon carcinoma cells (HT-29, CaCo2), poorly differentiated cells from lymph node metastasis of colon carcinoma (SW-620), chronic myeloid leukaemia in blast crisis (K562), T-cell leukaemia (Jurkat), T-cell lymphoma (HuT78) and aortic endothelial cells (HAEC). Human blood lymphocytes (lymphocytes) were derived from 10 healthy donors.

#### 4.2.2. Cell culturing

Cells, NCI-H358, HT-29, CaCo2, HeLa, MIAPaCa2, HEp-2, and SW-620 were grown as a monolayer in tissue culture flasks (250 ml; BD Falcon, Germany) in Dulbecco's modified Eagle medium (DMEM) with 10% foetal bovine serum (FBS) supplemented with 2 mM glutamine, 100 U of penicillin and 0.1 mg streptomycin.

Cells, K562, JURAT, HuT78, and lymphocytes were grown in RPMI-1640 medium supplemented with 10% FBS. Human aortic endothelial cells (HAEC) were grown in Medium 200 supplemented with serum growth supplements (Cascade Biologics). Cells were cultured in a humidified (95% air, 5% $CO_2$) $CO_2$ incubator (Shell Lab, Sheldon Manufacturing, USA) at 37 °C. The trypan blue dye exclusion method was used to assess cell viability.

#### 4.2.3. Cell growth inhibition assay

Cytotoxic effects on tumour cell growth were determined using the MTT assay.[27] In general, investigated compounds were dissolved in dimethylsulfoxide (DMSO) as a $1 \times 10^{-2}$ M stock. All working dilutions ($10^{-5}$–$10^{-8}$ M) were prepared immediately before each experiment in the water of highest purity. The solvent (DMSO) was also tested for eventual inhibitory activity by adjusting its concentration to be the same as in working concentrations. At day zero of the experiment tumour cells, $2 \times 10^4$ cells/ml, were plated onto 96-microwell plates (Greiner, Austria, EU) and allowed to attach overnight in a $CO_2$ incubator (Shell Lab, Sheldon Manufacturing, USA). Twenty four hours later, the medium was replaced with a fresh medium containing various well defined concentrations of investigated compounds. Controls were grown under the same conditions without the addition of the test substances. After 72 h of incubation medium was removed and 40 μl of MTT (5 mg/ml of phosphate buffered saline) was added. DMSO (160 μl) was added to each well to dissolve in water insoluble MTT-formazane crystals. The plates were transferred to an Elisa plate reader (Stat fax 2100, Pharmacia Biotech, Uppsala Sweden). The absorbency was measured at 570 nm on a microplate reader. All experiments were performed at least 3 times, with 3 wells each.

The percentage of cell growth (PG) was calculated by the following equation:

$PG = (A - A_{BLANCK}/A_{CONTROL} - A_{BLANCK}) \times 100$

BLANCK = medium without cells containing cytostatic and MTT.

#### 4.2.4. Fluorescence microscopy

Stock solutions of **1** and **2** ($c = 1$ mM) in DMSO were diluted to 1, 0.1 and 0.01 μM with DME medium. HeLa cells were grown on microscopic slides ($1 \times 10^5$ cells/slide) at 37 °C for 24 h. The three groups of tests were performed: **(1)** Cells were incubated with **1** or **2** (1–0.01 μM, in DME medium) for 5–120 min, washed with PBS, covered with a glass coverslip and analysed; **(2)** Control cells, in order to confirm the cells viability, were treated in propidium iodide (PI) solution (0.01 μM) for 60 min, washed with PBS and analysed under the microscope (PBS as mounting medium); **(3)** Cells were incubated with **1** or **2** ($c = 0.1$ μM, in DME medium) for

60 min, than washed with PBS and incubated in DAPI-methanol solution (1 nM) for 3 min at room temperature in the dark. DAPI-methanol solution was decanted, cells were rinsed with PBS, covered with a glass coverslip and analysed. The entry and intracellular distribution of tested compounds were analysed under the fluorescence microscope (Axioskop 2 MOT, Carl Zeiss Jena GmbH, Jena, Germany) with Zeiss filter combinations: (f3) BP 450–490, LP 520 for **1** and **2**; (f1) BP 365/12, FT 395, LP 397 for DAPI and (f2) BP 530–585, FT 600, LP 615 for PI.

## Acknowledgements

This research was supported by Grants of Croatian Ministry of Science, Education and Sport Nos.: 219-0982914-2176 and 098-0982914-2918. The authors wish to thank Mrs. Kristina Kalmar and Mrs. Anđelka Bugarin for excellent technical help in cell culturing.

## Supplementary data

Supplementary data associated with this article can be found, in the online version, at doi:10.1016/j.bmc.2009.04.070.

## References and notes

1. Trinquet, E.; Mathis, G. *Mol. Bio. Syst.* **2006**, *2*, 380.
2. Benson, S. C.; Mathies, R. A.; Glazier, A. N. *Nucleic Acids Res.* **1993**, *21*, 5720.
3. Benson, S. C.; Zeng, Z.; Glazier, A. N. *Anal. Biochem.* **1995**, *231*, 247.
4. Smith, L. M.; Sanders, J. Z.; Kaiser, R. J.; Hughes, P.; Dodd, C.; Connell, C. R.; Heiner, C.; Kent, S. B. H.; Hood, L. E. *Nature* **1986**, *321*, 674.
5. Prober, J. M.; Trainor, G. L.; Dam, R. J.; Hobbs, F. W.; Robertson, C. W.; Zagursky, R. J.; Cocuzza, A. J.; Jensen, M. A.; Baumeister, K. *Science* **1987**, *238*, 336.
6. Li, Y.; Glazer, A. N. *Bioconjugate Chem.* **1999**, *10*, 241.
7. Carnelly, T. J.; Barker, S.; Wang, H.; Tan, W.; Le, C. *Chem. Res. Toxicol.* **2001**, *14*, 1513.
8. Denijn, M.; Schuurman, H.-J.; Jacobse, K. C.; De Weger, R. A. *APMIS* **1992**, *100*, 669.
9. Wiegant, J.; Bezrookove, V.; Rosenberg, C.; Tanke, H. J.; Raap, A. K.; Zhang, H.; Bittner, M.; Trent, J. M.; Meltzer, P. *Genome Res.* **2000**, *10*, 861.
10. Lipshutz, R. J.; Fodor, S. P. A.; Gingeras, T. R.; Lockhart, D. J. *Nat. Genet. Suppl.* **1999**, *1*, 20.
11. Ferea, T. L.; Brown, P. O. *Curr. Opin. Genet. Dev.* **1999**, *9*, 715.
12. *DNA and RNA Binders*; Demeunynck, M., Bailly, C., Wilson, W. D., Eds.; Wiley-VCH: Weinheim, 2002.
13. Cantor, C. R.; Schimmel, P. R. In *Biophysical Chemistry*; WH Freeman and Co.: San Francisco, 1980; pp 1109–1181.
14. Wilson, W. D.; Ratmeyer, L.; Zhao, M.; Strekowski, L.; Boykin, D. *Biochemistry* **1993**, *32*, 4098.
15. (a) Timtcheva, I.; Maximova, V.; Deligeorgiev, T.; Zaneva, D.; Ivanov, I. *J. Photochem. Photobiol. A: Chem.* **2000**, *130*, 7; (b) Deligeorgiev, T.; Gadjev, N.; Timtcheva, I.; Maximova, V.; Katerinopoulos, H.; Foukaraki, E. *Dyes and Pigments* **2000**, *44*, 131; (c) Timtcheva, I.; Maximova, V.; Deligeorgiev, T.; Gadjev, N.; Drexhage, K. H.; Petkova, I. *J. Photochem. Photobiol. B: Biol.* **2000**, *58*, 130; (d) Deligeorgiev, T.; Maximova, V.; Timtcheva, I.; Gadjev, N.; Drexhage, K. H. *J. Fluoresc.* **2002**, *12*, 225; (e) Gadjev, N.; Deligeorgiev, T.; Timtcheva, I.; Maximova, V. *Dyes and Pigments* **2003**, *57*, 161; (f) Deligeorgiev, T.; Timtcheva, I.; Maximova, V.; Jacobsen, J. P.; Drexhage, K. H. *Dyes and Pigments* **2004**, *16*, 79.
16. Deligeorgiev, T.; Gadjev, N.; Vasilev, A.; Maximova, V.; Timtcheva, I.; Katerinopoulos, H.; Tsikalas, G. *Dyes and Pigments* **2007**, *75*, 466.
17. (a) Steiner-Biočić, I.; Glavaš-Obrovac, L.; Karner, I.; Piantanida, I.; Žinić, M.; Pavelić, J.; Pavelić, K. *Anticancer Res.* **1996**, *16*, 3705; (b) Marczi, S.; Glavaš-Obrovac, L.; Karner, I. *Chemotherapy* **2005**, *51*, 217; (c) Marczi, S.; Glavaš-Obrovac, L.; Belovari, T.; Stojković, R.; Ivanković, S.; Šerić, V.; Piantanida, I.; Žinić, M. *Cancer Chemother. Pharmacol.* **2008**, *62*, 595.
18. McGhee, J. D.; von Hippel, P. H. *J. Mol. Biol.* **1976**, *103*, 679.
19. Jain, S. C.; Sobell, H. M. *J. Biomol. Struct. Dyn.* **1984**, *1*, 1179.
20. Nitta, Y.; Kuroda, R. *Biopolymers* **2005**, *81*, 376.
21. Martinez, R.; Chacón-García, L. *Curr. Med. Chem.* **2005**, *12*, 127.
22. Cooper, T. M. *Ther. Clin. Risk Manag.* **2007**, *3*, 1135.
23. Luchetti, F.; Gregorini, A.; Papa, S.; Burattini, S.; Canonico, B.; Velentini, M.; Falcieri, F. *Haemalogica* **1998**, *83*, 974.
24. Hoffman, M. R.; Connors, K. M.; Meerson-Monosov, A. Z.; Herrera, H.; Price, J. H. *Proc. Natl. Acad. Sci.* **1989**, *86*, 2013.
25. Chaires, J. B.; Dattagupta, N.; Crothers, D. M. *Biochemistry* **1982**, *21*, 3933.
26. Malojčić, G.; Piantanida, I.; Marinić, M.; Žinić, M.; Marjanović, M.; Kralj, M.; Pavelić, K.; Schneider, H.-J. *Org. Biomol. Chem.*, **2005**, *3*, 4373.
27. Mickisch, G.; Fajta, S.; Keilhauer, G.; Schlick, E.; Tschada, R.; Alken, P. *Urol. Res.* **1990**, *18*, 131.